Optimizing biobased thermoset resins by incorporating cinnamon derivative into acrylated epoxidized soybean oil

Diego Lascano , Jaume Gomez-Caturla , David Garcia-Sanoguera , Daniel Garcia-Garcia , Juan Ivorra-Martinez *

Institute of Materials Technology (ITM), Universitat Politècnica de València (UPV), Plaza Ferrándiz y Carbonell 1, 03801, Alcoy, Alicante, Spain

ABSTRACT

The study successfully developed thermoset materials utilizing acrylate epoxidized soybean oil (AESO) and allyl cinnamate (ACIN) with *tert*-butyl peroxybenzoate (TBPB) as the initiator. Isothermal curing at temperatures between 110 °C to 140 °C of the developed formulations, showed that higher temperatures accelerated the conversion process. The higher curing temperature increased the degree of conversion, leading to obtain the best flexural strength for samples cured at 130 °C. However, samples cured at 120 °C exhibited better impact properties due to a lower degree of conversion, which allows for a more mobile reticular network. In addition, morphological observations confirmed these mechanical property trends. Dynamic thermal characterization revealed changes in glass transition temperature and exothermic reactions due to unreacted products appeared for materials cured at low temperature. Increasing curing temperature allowed to enhance thermal stability by increasing molecular weight. Finally, thermomechanical analysis confirmed stiffness and glass transition temperature increases observed during flexural tests and thermal characterization.

1. Introduction

The new paradigm endorsed by governments aims to advance the research of alternative materials that are less environmentally detrimental. Polymeric materials, predominantly derived from non-renewable sources such as petroleum, contribute significantly to pollution during their transformation into raw materials, exacerbating global warming issues [1–3]. In response to this challenge, numerous strategies have been proposed to replace current petroleum-based materials with alternatives that are more environmentally friendly. The exploration of biobased materials has captured the attention of both researchers and industries, seeking to develop materials that match the performance of existing ones but originate from more sustainable and eco-friendly sources [4,5].

A significant portion of contemporary polymeric materials comprises thermoset materials, distinguished by a crosslinking process that establishes a reticular network of polymeric chains. Thermosets are predominantly derived from petroleum-based resources, boasting exceptional properties that render them appealing for various applications. The crosslinked networks formed during the reaction grant thermoset materials outstanding thermal and dimensional stability, setting

them apart from thermoplastic materials [6,7]. Consequently, these polymeric materials find widespread application in diverse sectors including industrial coatings, adhesive formulations, and the development of fiber-reinforced materials for high-performance applications [8,9]. Epoxy is the most commonly used thermoset matrix for fiber-reinforced composites due to its exceptional properties. However, alternative options such as polyester resins also exhibit noteworthy properties that make them valuable for composite material development [10,11].

The development of epoxy resins involves the use of diglycidyl ether of bisphenol A (DGEBA). In the condensation process for obtaining DGEBA, bisphenol A (BPA) and epichlorohydrin (ECH) undergo a reaction in the presence of sodium hydroxide (NaOH). However, it is noteworthy that, besides their non-renewable origin, both BPA and ECH are associated with adverse effects on living organisms. BPA is derived from petroleum-based phenol and benzene, while ECH is produced from 1-chloropropane with glycerol. In an effort to replace current epoxy resins, various materials have been explored as substitutes for the petroleum-based monomers. Examples include epoxidized plant oils, isosorbide, caranol, derivatives from lignin, itaconic acid, and vanillin, among others. These alternatives aim to mitigate the environmental

---

impact associated with the production of epoxy resins and contribute to the development of more sustainable and eco-friendly materials. [12,13].

The formation of biobased thermoset materials requires the selection of an oil with an unsaturated structure containing highly reactive functionalities, such as carbon–carbon double bonds [14]. Given the intrinsic appeal, the development of biobased materials has garnered significant interest in society. Notably, soybean oil derivatives have emerged as a focal point. Epoxidized soybean oil (ESO) stands out as the most extensively investigated raw material for the synthesis of epoxy resins (EP) [15]. An alternative approach involves subjecting ESO to an acrylation process, resulting in acrylated epoxidized soybean oil (AESO) [16]. While this material forms a thermoset through radical polymerization, it exhibits suboptimal mechanical properties and low glass transition temperatures. These shortcomings arise from its chemical structure, characterized by three long chains and a low carbon–carbon double bonding density. The incorporation of styrene can enhance bonding abilities but introduces toxicity concerns [17]. An illustrative instance of biobased thermoset materials derived from soybean oil is exemplified in the work of Pansumdaeng *et al.* In their research, the developed thermoset material demonstrated exceptional properties conducive to the creation of triboelectric nanogenerators for sustainable power generation. The material exhibited outstanding thermal stability and low water uptake properties, highlighting its potential for environmentally friendly applications [18]. It has to be highlighted that AESO can be applied a biobased material for many applications such coatings, thermoset materials among others providing functionalities like the antibacterial ability [19,20].

Considerable efforts have been directed towards substituting the styrene content in biobased thermoset resins with alternative reactive diluents that are less toxic or sourced from renewable origins [21]. The introduction of a reactive diluent allows to improve the ability to crosslinking ability of the material, mixtures with lower viscosity have a higher mobility that helps the rearrangement process during the curation process [22]. In addition, the adjustment of viscosity becomes imperative in certain applications due to the high viscosity of the monomers before the curing process. Significantly, reducing the viscosity of uncured thermoset materials holds strategic importance in facilitating fiber impregnation. This reduction enhances fiber impregnation, consequently improving the overall properties of the composite material [23]. Several examples of biobased reactive diluents include furfural-based products derived from renewable resources such as wood and cereals. FOM (2-[(oxiran-2-ylmethoxy)methyl]furan), also known as furfurylglycidyl ether (FGE), has proven successful as a reactive diluent for epoxy resin. The incorporation of FGE results in viscosity reduction of the resin. Additionally, the use of this diluent leads to a decrease in the number of effective epoxy groups, thereby limiting the crosslinking process [24]. Another viable option for biobased reactive diluents involves allyl-based monomers. The inherent reactivity of this group promotes the crosslinking process, contributing to an enhancement in thermal stability [25].

The polymerization process of the monomers in thermoset materials necessitates the initiation of the reaction through the addition of an initiator. These initiators are activated by an external energy input, which can be applied through various means such as heat, UV light, or temperature variations [26,27]. Upon receiving the external energy, the initiator undergoes decomposition, generating free radicals that initiate the crosslinking process, leading to the formation of larger macromolecules. Throughout this process, the viscosity of the material gradually increases until a transition from a liquid-like phase to a solid state occurs, ultimately defining the final form of the thermoset material [28]. Most of the employed initiators are based on peroxides that start its decomposition creatin alkoxyl radicals that attack the employed monomers [29].

This study introduces an innovative approach to the development of epoxy thermoset materials using AESO and allyl cinnamate, diverging from conventional petrochemical-based resins. Integrating biobased components, this research supports global sustainability initiatives, addressing the critical demand for environmentally friendly materials in science. Allyl cinnamate serves a dual role, it mitigates environmental concerns due to its biobased origin and acts as a reactive diluent. This novel application of biobased reactive diluents improve processability without compromising performance. Enhanced processability promotes wider use of these materials in the production of biobased composites, facilitated by decreased viscosity that aids in fiber impregnation. This allows for their use in the design of fiber-reinforced objects. The study conducts a thorough examination of the curing process, identifying optimal temperatures through differential scanning calorimetry (DSC) and chemical extraction methods, which assess the unreacted fractions in the samples. Various temperatures and durations were applied during the curing process, and the resultant properties were systematically evaluated. The mechanical properties of the samples were rigorously tested, and the surface morphology of the fractures was analyzed to gain deeper insights into the material's structure. Overall, this investigation challenges traditional material choices and enhances understanding of the curing processes, setting a foundation for future innovations in biobased thermosets designed for high-performance applications.

2. Experimental

2.1. Materials and sample manufacture

Epoxidized acrylate soybean oil (AESO) with CAS Number 91722–14-4 was procured from Sigma Aldrich (Lyon, France). As a diluent, allyl cinnamate (ACIN) with a purity exceeding 99 %, identified by CAS Number 1866–31-5, was sourced from Sigma Aldrich (Steinheim, Germany). The initiator *tert*-butyl peroxybenzoate (TBPB), possessing a purity above 95 % and characterized by CAS Number 614–45-9, was obtained from Sigma Aldrich (Schnelldorf, Germany). The chemical structure of each material employed is depicted in Fig. 1. All materials were utilized as received without further modifications.

For thermoset preparation a consistent ratio of 2:1 in weight for AESO to ACIN was maintained in all cases. The selected materials (AESO and ACIN) for this work have in both cases doble bonds (blue, green and red spots) as can be observed in Fig. 1. As will be observed later in this work, these double bonds will play an important role in the crosslinking formation. In order to start the reaction, the initiator at a ratio of 2 phr (per hundred resin) was introduced.

The crosslinking process was initiated through the thermal decomposition of the initiator. Uncured materials were placed in an oven at varying temperatures and durations to evaluate the impact of the curing process on the outcomes of the developed thermoset materials. Temperature ranges from 110 °C to 140 °C were explored in this study. Regarding curing time within the oven, two levels were considered: 1.5 h and 2.5 h. Sample designations include both the oven temperature and the corresponding curing time. For instance, a sample cured at 130 °C for 2.5 h is denoted as 130/2.5. The parameters chosen for the curation process are determined based on the decomposition characteristics of the selected initiator. Specifically, for TBPB (*tert*-Butyl peroxybenzoate), the half-life of decomposition at a temperature of 122 °C is approximately 1 h. When the temperature is elevated to 142 °C, this duration significantly decreases to approximately 0.1 h [30].

2.2. Curing study

The uncured thermoset material underwent thermal analysis using a DSC 25 instrument from TA Instruments (New Castle, United States of America). The thermal program initiated at 40 °C and increased at a rate of 80 °C/min until reaching the designated curing temperature. This temperature was maintained for 90 min to quantify the heat released by the sample during the curing process. Throughout the curing process, a continuous flow of nitrogen at a rate of 50 mL/min was maintained, and
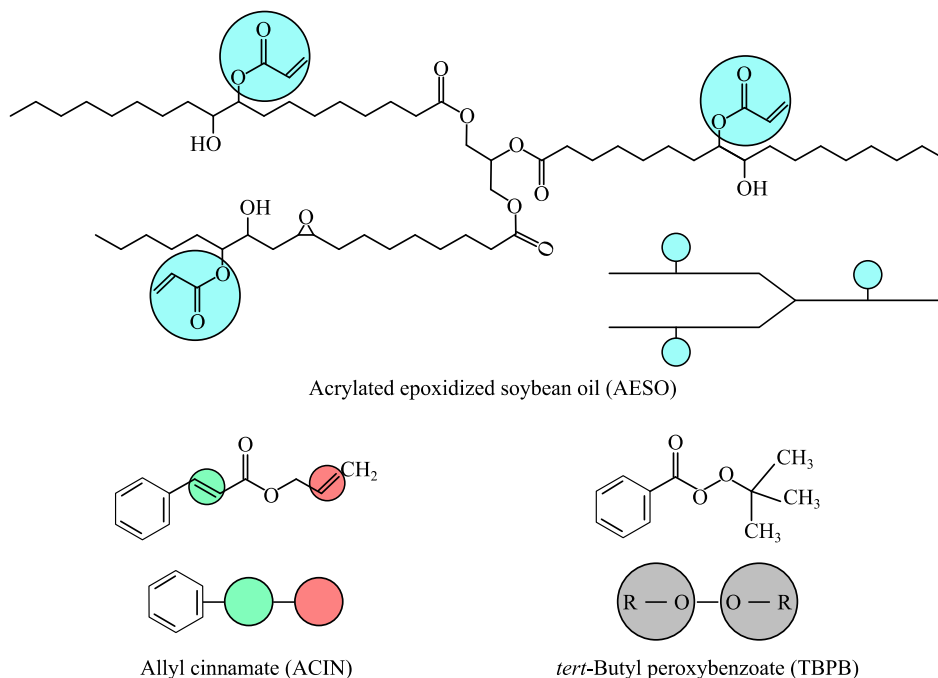
Acrylated epoxidized soybean oil (AESO)

Allyl cinnamate (ACIN)

tert-Butyl peroxybenzoate (TBPB)

Fig. 1. Chemical structure of the products employed in the biobased thermoset obtention with the potential reaction points.

the sample weight ranged between 5 and 6 mg. The degree of conversion (α) of the sample was calculated using the following formula:

$$\alpha\,(\%) = \frac{\Delta h}{\Delta h_T}\,\text{\^A}\cdot 100 \qquad (1)$$

where:

Δh is the measured enthalpy under isothermal conditions.

Δh_T is the measured enthalpy for the thermoset material cured in dynamic conditions, utilizing a heating ramp from 40 °C to 250 °C at 2 °C/min.

Additionally, for the analysis of the curing process, 1 g of the cured thermoset material underwent a 24-hour immersion in 15 mL dichloromethane to facilitate an extraction process. This extraction process enables the removal of the uncured fraction from the sample, allowing for the calculation of the gel fraction using the following equation:

$$\text{Gel fraction}\,(\%) = \frac{m_f}{m_i}\,\text{\^A}\cdot 100 \qquad (2)$$

where:

m_f is the weigh of the sample after the extraction process.

m_i is the initial mass of the sample.

2.3. Chemical study

The chemical composition analysis of the primary constituent of the thermoset material and the resulting thermoset materials under various curing conditions was conducted using a Fourier-transform infrared (FT-IR) spectrometer. A Spectrum Two FT-IR Spectrometer from Perkin Elmer (Waltham, United States of America) was employed for this purpose. The obtained data represent the average of ten scans across a spectral range of 4000 to 500 cm^{-1}, with a spectral resolution set at 4 cm^{-1}.

2.4. Mechanical properties

The assessment of flexural properties involved a three-point bending test conducted in accordance with ISO 178:2019 standards. Specimens with dimensions of 80 × 10 × 4 mm^3 and a span length of 64 mm were used for the test. The ELIB 50 universal testing machine manufactured by S.A.E. Ibertest (Madrid, Spain), configured appropriately for flexural measurements, was employed for the measurements. The tests were conducted at a crosshead speed of 5 mm/min, utilizing a 5 kN load cell. The main parameters in the measurement include: the flexural strength (σ_f), strain at failure (ε_f) and flexural modulus (E_f). Five samples were tested for each material.

The assessment of impact strength was performed through the Charpy impact test following ISO 179–1:2010 standards. A 80 × 10 × 4 mm^3 specimen was utilized for this test, and the impact testing apparatus consisted of a Charpy pendulum provided by Metrotec S.A. (San Sebastian, Spain), equipped with a 1 J pendulum. Five samples were tested for each material.

Hardness measurements were conducted using a 76-D hardness tester from J. Bot Instruments (Barcelona, Spain), utilizing the Shore D scale with a stabilization time of 15 s in accordance with ISO 868:2003. Five measurements were made in each material.

2.5. Morphological properties

Field emission scanning electron microscopy (FESEM) was employed to analyze the fracture surface obtained in the impact test. The examination was conducted using a ZEISS ULTRA 55 microscope from Oxford Instruments (Abingdon, UK). In preparation for the analysis, the samples used in the impact test underwent a specific process. A layer of gold and palladium alloy was applied using an EMITECH sputter coating SC7620 from Quorum Technologies, Ltd. (East Sussex, UK) to ensure a conductive surface, which is crucial for the proper functioning of this microscopy technique. Subsequently, the prepared samples were introduced into the microscope, applying a voltage of 2 kV for imaging.

2.6. Thermal properties

The thermal properties of the cured materials were assessed through differential scanning calorimetry (DSC) using a DSC 25 instrument from TA Instruments (New Castle, United States of America). The thermal measurement program initiated at 40 °C and included a cooling process

down to −80 °C, followed by a heating program up to 250 °C. All stages were executed at a rate of 5 °C/min with a constant nitrogen flow of 50 mL/min, and the sample weight ranged between 5 and 6 mg. Key parameters extracted from this test include the glass transition temperature (T_g), the realized enthalpy during the curing process (Δh) and the temperature at peak maximum (T_p). Three replicates were performed for each sample.

Thermogravimetric analysis (TGA) was employed to determine thermal degradation parameters. The TGA characterization was conducted using a TG-DSC2 thermobalance from Mettler-Toledo (Columbus, OH, USA). A heating step ranging from 30 °C to 700 °C at a rate of 10 °C/min was applied under an air atmosphere. Analyzed parameters encompassed the temperature at which a 5 % mass loss occurred ($T_{5\%}$), the maximum degradation rate (T_{max}) measured from the first derivative of the weight loss curve, and also the residue mass at 700 °C. Three replicates were performed for each sample.

2.7. Thermomechanical properties

Dynamic mechanical thermal analysis (DMTA) was conducted using a Mettler-Toledo DMA1 instrument (Columbus, OH, USA) operating in a single cantilever mode. Specimens with dimensions of 20 × 5 × 2 mm3 were utilized, featuring a maximum deflection of 10 μm and an oscillation frequency of 1 Hz. The heating cycle ranged from −100 °C to 120 °C, with a heating rate of 2 °C/min. The results were analyzed in terms of storage modulus (E') and loss factor (tan δ). Three samples were tested for each material.

3. Results

3.1. Curing study

The crosslinking process of the AESO/ACIN thermoset material was carried out under isothermal conditions at different temperatures. Fig. 2 presents the evolution of the heat flow measured in DSC, along with the degree of conversion of the sample within the DSC. Table 1 compiles the key parameters extracted from the isothermal DSC test and the chemical extraction process. The results illustrate the significant influence of temperature on the heat flow and the degree of conversion of the various developed materials. The activation of the initiator necessitates external energy input to initiate the reaction. After the reaction start, it is proposed that multiple reaction occur at the same time and most of the times it is observed as a single reaction process [31]. Despite this is generally proposed, in this work the isothermal temperature of 130 °C
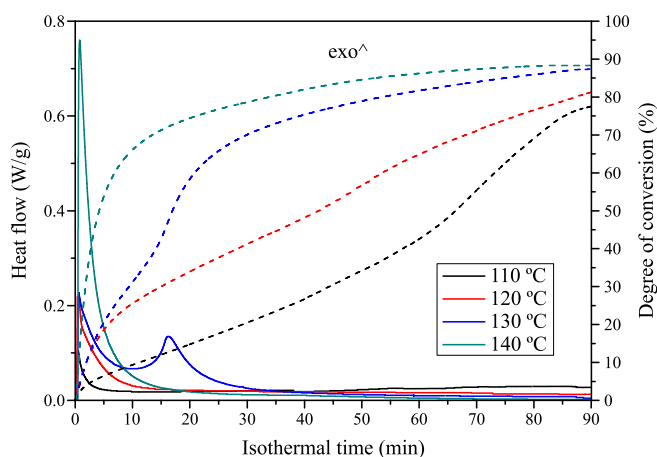

Fig. 2. Results from the isothermal DSC test for the uncured resin at different temperatures. Continuous lines indicate the heat released by the sample during the curing process and dashed line show the evolution of the degree of conversion.

Table 1
Main parameters of the curation process at different isothermal temperatures during 90 min in DSC and gel fraction by means of chemical extraction.

Sample	Δh(J/g)	α_{max} (%)	Gel fraction (%)
Dynamic conditions	201.6	–	–
Isothermal at 110 °C	160.7	77.7	76.4
Isothermal at 120 °C	163.4	81.0	80.3
Isothermal at 130 °C	175.0	86.8	85.6
Isothermal at 140 °C	178.8	88.6	87.9

proposed a dual peak process that suggest that a secondary reaction occurs after 10 min of isothermal treatment. The linearity of the reaction is sometimes lost due to the increase in the reaction rate that promotes a reduction in terms of reactant concentration and also an increase in the viscosity as proposed by XuFeng *et al.* [32]. Under the conditions proposed by XuFeng *et al.* the DSC curves obtained exhibited a dual peak similar to the one observed in this case. In this work, the kinetics of the reaction coupled with the changes in the viscosity of the mixture promotes the appearance of the dual peak only in the 130 °C isothermal conditions.

Higher isothermal temperatures led to increased heat at the outset of the reaction, triggering a pronounced change in the degree of conversion. After 90 min under the specified isothermal conditions, the degree of conversion measured in DSC reached 88.6 %, while the extraction of unreacted materials from the sample revealed a gel fraction of 87.9 %.

Post the initial reaction, the degree of conversion curve exhibited an asymptotic behavior, indicating a slower change in the degree of conversion over the tested time. The curve shapes observed in this study bear resemblance to those obtained in other works, such as Monteseón *et al.* investigation of the curing of an epoxy-amine thermoset system. Monteseón *et al.* explored temperature distribution based on sample thickness, emphasizing that variations in temperature lead to differences in material properties [33].

The variation in the isothermal temperature employed in the process results in a corresponding reduction in the heat flow over the tested time. This reduction indicates lower conversion, reflecting a change in the sample's behavior. The curves exhibit an asymptotic behavior, particularly in the samples cured at higher temperatures, suggesting that, under the proposed conditions, the formulation cannot achieve full conversion. It's important to note that the enthalpy considered for full conversion is calculated based on this material subjected to a dynamic DSC test ending at 250 °C. Achieving complete conversion would likely require an increase in the process temperature. However, in this study, a decision was made not to escalate temperatures beyond 130 °C due to the observed fragility in the samples. The fragility observed in samples above 130 °C poses challenges to the testing process. This incomplete conversion of monomers is not unique to this work and is observed in other studies. Anusic *et al.* work on a thermoset material made of ELO and citric acid is an illustrative example of materials that could not achieve full conversion under certain temperature conditions [34].

The result of the curing process at 110 °C suggests that the AESO/ACIN thermoset material attains a degree of conversion of approximately 77.7 %. This result aligns with the gel fraction measurement, yielding a value of 76.3 %. However, this reduced crosslinking process, as will be discussed later, leads to a material with low mechanical properties, combining low resistance with low ductility. The presence of an uncured structure results in a low molecular weight, contributing to inferior mechanical properties. Changes in molecular weight also affect other properties, such as the glass transition temperature of the sample. Increasing the crosslinking density is crucial for obtaining the desired material properties. In Lu *et al.*'s work, an improvement in the strength and ductility of thermoset materials based on modified soybean oil was achieved with an increase in curing time [35].

The crosslinking process, as analyzed above, warrants a detailed examination, with a focus on free radical formation in each material, as

depicted in Fig. 3. Subsequent to radical formation, Fig. 4 illustrates the interaction of each monomer. The initiator employed is TBPB, a peroxide that decomposes into two parts, generating a free electron in each part. These free electrons can interact with the double bonds present in AESO and ACIN. In the case of AESO (indicated by the blue spot), which possesses a double bond in the acrylic group, the peroxide interaction leads to the attack of the double bond, creating a free electron. As for the double bonds in ACIN, there are two possibilities for interaction with TBPB, represented by the red and green spots.

Following free radical formation, an addition polymerization process takes place, as illustrated in Fig. 4. The free electrons in each monomer interact with other free electrons, leading to the creation of new bonds between each monomer. Various possible interactions can occur in this process. The new bonds may form between two different AESO chains, transforming the oil into a thermoset material. However, the properties of this material may be limited due to the high viscosity resulting from the formation of bonds between the acrylic groups. Another possible interaction involves the formation of a bridge between two AESO chains and one ACIN molecule, connecting them at the two proposed points (green and red spots). Additionally, interactions between two ACIN chains can also occur in this process. It has to be highlighted that the presence of the new permanent covalent bonds, promote an insoluble and infusible material that can not be re-shaped for its recyclability [36].

AESO can self-polymerize by free radical polymerization as it has been reported by Zhang et al. [37], with just 0.5 wt% N-tertbutyl peroxybenzoate as initiator. As AESO is a rather viscous resin, it needs previous heating to ensure good mixing with the initiator. On the other hand, allyl cinnamate, as other cinnamic acid derivatives can undergo homopolymerization with different routes, as reported by Hang-Thi et al. [38], who synthesized poly(4-hydroxycinnamic acid) (P4HCA) by thermal polycondensation. In the case of cinnamate, the homopolymerization process can be initiated either by peroxides or UV radiation. Karthaus et al. [39] reported the crosslinking of different polycinnamates by using UV radiation thus corroborating the potential of the unsaturations to form crosslinked structures. Polycinnamates can also be self-polymerized by group-transfer polymerization (GPT), as described by Imada et al. [40], who reported the synthesis of polycinnamates from methyl, ethyl, isopropyl, and methyl 4-methyl cinnamates using 1-methoxy-1-(trimethylsiloxy)-2-methyl-1-propene (MTS) as an initiator. It has also been reported the synthesis of poly(ethyl cinnamate) homopolymers by heating or by a free radical initiated addition process with 2,2′-azobisisobutyronitrile (AIBN) or t-butylperoxybenzoate initiators [41,42]. As it happens with unsaturated polyester resins (UP), a reactive diluent (usually styrene) is required to tailor the desired viscosity and hence, allowing manufacturing processes. Recently, new biobased reactive diluents such as terpenes and cinnamates, have been proposed for industrial UP resins [43]. Despite cinnamates offer low reactivity due to the low reactivity of the unsaturation derived from cinnamic acid, allyl esters of cinnamic acid, provides extra reactivity due to the unsaturation located in terminal position. Thus, allyl cinnamate could play a

key role in reducing the viscosity of AESO resin (diluent), as well as act as a comonomer (reactive) in AESO/cinnamate crosslinked polymers initiated by organic peroxides. The organic peroxide decomposes at relatively low-moderate temperatures leading to free radical formation. These free radicals can easily react with available unsaturations (mainly on acrylic groups contained in AESO, and allyl group in cinnamate) thus promoting copolymerization by free radical addition in a similar way to conventional vinylester resin (VE) with styrene. It is important to bear in mind that the reactivity of the allyl group in cinnamate is similar to that of a conventional styrene in UP and VE resins, while the b) mechanism of free radical formation indicated in Fig. 4, related to ACIN, is not as favored as the a) mechanism of the allyl group, due to steric hindrance.

3.2. Chemical study

The chemical characterization of the AESO/ACIN materials developed is depicted in Figs. 5 and 6. Beginning with the materials utilized for the thermoset development, the primary component is AESO, exhibiting characteristic peaks at 3460 (–OH groups), 1731 (C = O), and 1241 cm^{-1} (C–O), which represent the main polar constituents of AESO molecules. The peaks originating from the C–O–C stretching vibration of esters are situated at 1160 and 1092 cm^{-1}. Additionally, several peaks at 2921 and 2853, and 1457 and 1378 cm^{-1} are attributed to the asymmetric stretching vibrations and deformation of C–H [44]. Lastly, the peak at 811 cm^{-1} corresponds to the epoxy groups that are still present in the acrylated oil [45,46].

Regarding the reactive diluent employed in the manufacturing process, ACIN displays characteristic peaks, particularly the ethylbenzene with multiple peaks located at 2886, 2942, 2975, 3039, and 3075 cm^{-1}, which can be associated with the ring CH vibrations [47]. Additionally, the C = O peak at 1731 cm^{-1} and the C = C bond at 1637 cm^{-1} facilitate the reaction with the AESO chains.

The initiator used also exhibits multiple peaks for ethylbenzene between 2886 and 3075 cm^{-1}. Furthermore, the most significant peak of the initiator is the O-O bond, which is around 850 cm^{-1}, albeit with very low intensity, making its observation challenging [48]. As expected, the mixture without curing exhibits the same peaks as those present in the raw materials used. Given that AESO is the primary component, these peaks hold the highest relevance in the measured spectra.

When comparing the uncured resin with the AESO/ACIN thermoset material, discernible differences are observed in the peak near 1600 cm^{-1}, which represents the double bond C = C. During the isothermal process, these double bonds undergo breakdown due to the action of TBPB. As indicated in the curing study, higher temperatures facilitate a greater level of conversion, resulting in the breakdown of a higher amount of double bonds and subsequently reducing the intensity of this peak. This observation aligns with the findings of Su et al., who also noted a reduction in this peak with an increase in the curing temperature [49]. As suggested, the primary mechanism of reaction involves the acrylic groups. However, another potential point of reaction is the epoxy
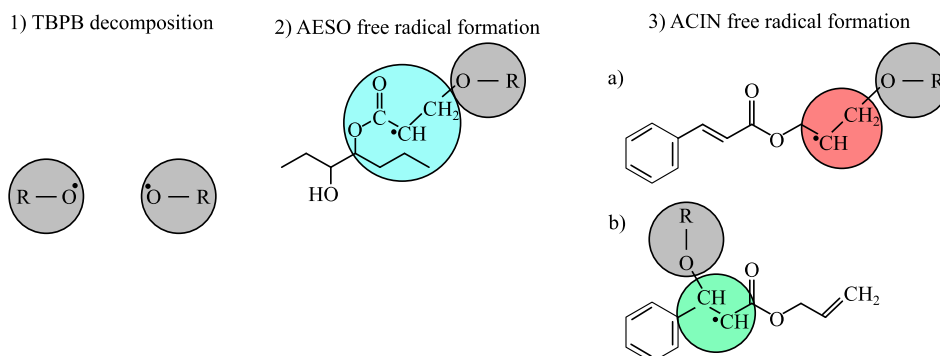

Fig. 3. Free radical formation with the TBPB decomposition in the acrylic group and the ACIN.
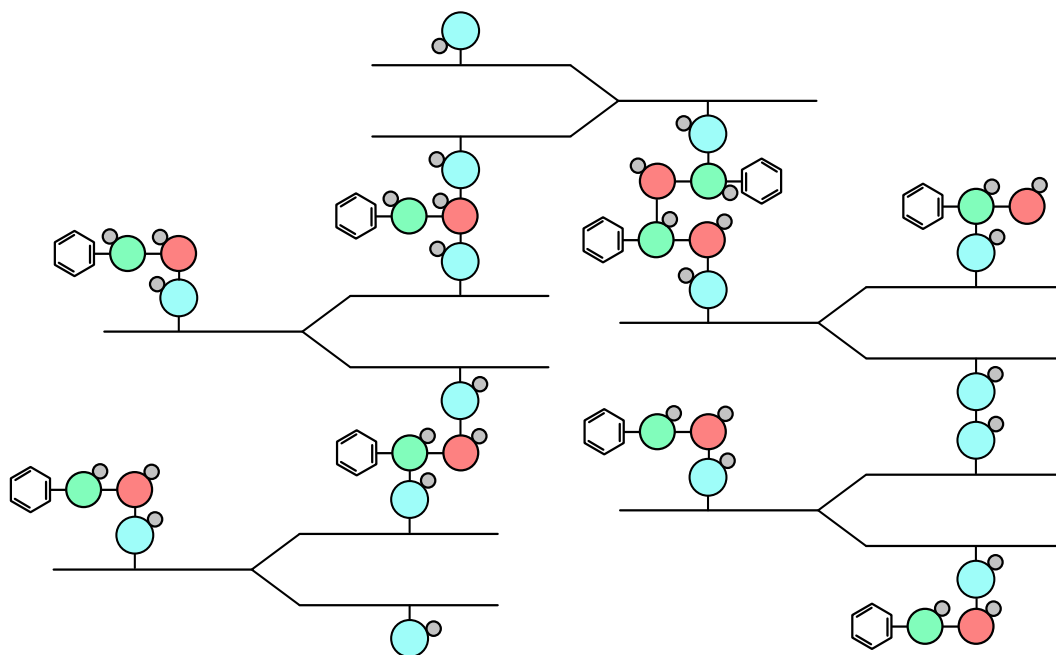
Fig. 4. Representation of the reticular structure obtained by the crosslinking reaction of AESO/ACIN. Blue spots represent the acrylic group of AESO, green/red spots represent the possible reaction points in ACIN and grey spot represent the decompose peroxide. (For interpretation of the references to colour in this figure legend, the reader is referred to the web version of this article.)
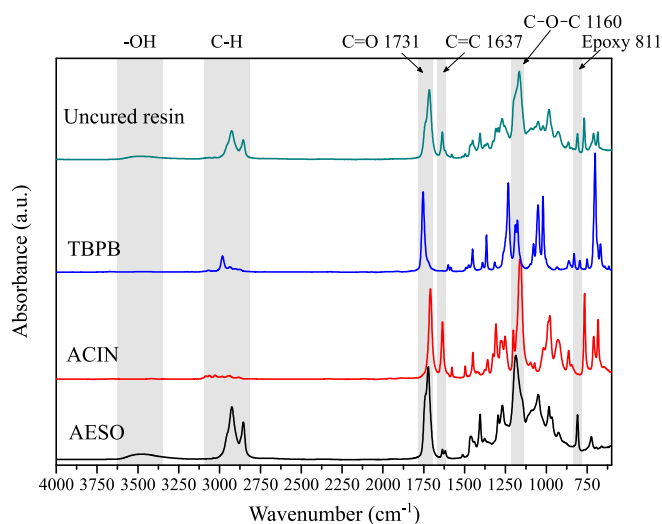

Fig. 5. FTIR-ATR spectra of the materials employed for the AESO/ACIN obtention and uncured the mixture.

Fig. 6. FTIR-ATR spectra of the cured thermoset AESO/ACIN for different isothermal temperatures.

group in the AESO chains. The peak at 811 cm^{-1} corresponding to epoxy groups diminishes with the increase in curing temperature. Mauro *et al.* observed a similar phenomenon in the manufacturing of thermoset resins with epoxidized vegetable oils, suggesting a polymerization of ESO chains occurred [50].

3.3. Mechanical properties

The mechanical performance of the AESO/ACIN thermoset materials is detailed in Table 2, illustrating various samples subjected to different isothermal conditions and curing times. Notably, the flexural strength of the samples exhibits differences concerning resistance and ductile behavior. Specifically, the lowest strength is observed in samples cured at the lowest temperature of 110 °C, where the flexural strength falls below 3 MPa. At this temperature, the crosslinking reaction is relatively
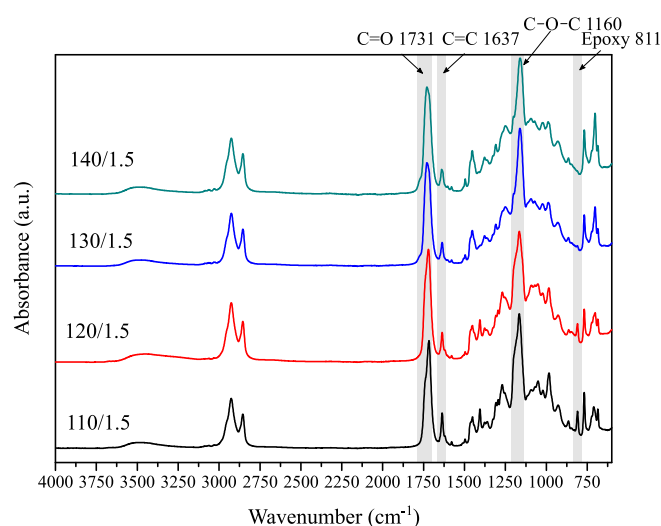
minimal, thereby diminishing mechanical performance. Conversely, above 130 °C, the samples display a highly brittle behavior, hindering proper sample cutting for testing, and thus, flexural and impact strength tests could not be conducted, rendering no available data. The employed reactive diluent employed can act in two ways in the thermoset material. In those cases that the AC chains react with other chains to create a solid material contributing to obtain a solid and stiff material. The other chains that do not react by the conditions proposed can act as a plasticizer improving the ductility of the material [22]. In addition, free chains submitted to high temperatures for a long time can volatilize promoting the fragilization of the samples. The employed reactive diluent has a boiling point of 289 °C but the volatilization of the allyl cinnamate starts at a lower temperature as observed by Barandiaran *et al* in the thermoplastic formulations developed with the ACIN [51]. For

Table 2

Main mechanical properties obtained from flexural test, Charpy impact test and Shore D harness test for the cured resins at different isothermal temperatures and times.

Sample	σ_f (MPa)	ε_f (%)	E_f (MPa)	Impact strength (kJ/m²)	Shore D harness
110/1.5	1.6 ± 0.2	5.1 ± 0.3	361 ± 20	5.6 ± 0.5	30.2 ± 0.8
110/2.5	2.7 ± 0.3	7.2 ± 0.6	431 ± 39	9.7 ± 0.8	40.0 ± 0.7
120/1.5	3.3 ± 0.4	7.3 ± 0.2	720 ± 24	12.1 ± 1.0	44.5 ± 0.8
120/2.5	6.1 ± 0.1	8.9 ± 0.4	801 ± 31	12.7 ± 0.9	46.6 ± 0.5
130/1.5	6.2 ± 0.5	10.0 ± 0.5	981 ± 26	3.2 ± 0.4	45.8 ± 0.5
130/2.5	6.4 ± 0.3	11.5 ± 0.7	926 ± 27	1.6 ± 0.6	48.7 ± 0.6
140/1.5	–	–	–	–	46.7 ± 0.6
140/2.5	–	–	–	–	49.5 ± 0.6

this reason, the developed thermosets materials that were cured at 140 °C were not able to test due to the high fragility exhibited.

The optimal output of a thermoset material is significantly influenced by the temperature employed. For instance, Sivasankaraiah *et al.* investigated different post-cure temperatures of composite materials comprising epoxy resin and glass fiber. They found that the flexural strength reached a maximum at 140 °C, with higher temperatures leading to a decrease in strength [52]. As the crosslinking network increases with temperature, prolonged exposure to high temperatures results in depolymerization, highlighting the presence of an optimum point. Another noteworthy difference in strength properties is the alteration in sample stiffness. A higher degree of curing fosters an increase in the flexural modulus due to a greater number of covalent bonds between involved chains, consequently restricting deformation and augmenting stiffness. For instance, the AESO/ACIN samples exhibited a flexural modulus increase from 361 MPa for samples cured at 110 °C for 1.5 h to 926 MPa for samples cured at 130 °C for 2.5 h. Similarly, changes in tensile modulus with varying degrees of curing have been documented by other researchers, such as Wan *et al.*, who reported an increase in tensile modulus due to the formation of new bonds during the curing process [53]. Moreover, alongside the enhancement of resistance properties, ductile properties like flexural elongation at break also increase with rising curing temperature. This observation aligns with findings from Daissè *et al.* regarding epoxy resins, where an increase in tensile and ductile properties coincided with higher curing conditions [54]. Additionally, the deformation of the sample before breakage benefits up to 130 °C. However, it's common for increased curing degrees to reduce elongation, as a higher number of bonds restricts chain mobility, contributing to the aforementioned improvements in flexural strength and modulus. Despite these variations, in cases where the degree of conversion of samples is low, an increase in covalent bonds comprising the reticular network aids in enhancing this parameter. This effect was also observed by Anusic *et al.*, who noted an increase in elongation at break for samples cured at the highest temperature and longest time [34]. Conversely, achieving a low degree of conversion results in uncured parts with a non-solid state, unable to support flexural efforts. An important effect to notice is that the possibility that the reactive diluent can also be acting as a plasticizer in the polymer matrix. This means free cinnamate chains allow samples have a greater ability to deform, allowing to improve the ductile properties. These findings have been also observed by Ribca *et al.* that obtained a lower stiffness despite an increase in terms of crosslinking density [55].

Regarding the impact strength of the samples, the increase in the employed isothermal temperature also significantly influences the sample outcomes. Higher isothermal temperatures lead to an increase in

the reticular network, with the most favorable outcome observed for samples cured at 120 °C. Lower temperatures result in weaker samples with low impact strength, breaking with minimal energy absorption. Conversely, higher temperatures yield a rigid network that hinders proper energy absorption during testing, resulting in very low impact strength values. As noted by Li *et al.*, the characterization of thermoset materials typically yields low impact strength values, with higher curing temperatures exacerbating sample brittleness [56].

The last mechanical property measured is the hardness of the samples. In this case, hardness could be measured up to 140 °C as the brittleness of these materials did not hinder the measurement. Since the hardness of the AESO/ACIN materials is linked to the material's resistance to penetration, this property follows the same trend as the material's stiffness. As the crosslinking density increases, so does the measured hardness of the materials. Grimalt *et al.* observed a similar effect for an unsaturated polyester resin cured with different reactive diluents [43].

3.4. Morphological properties

The observed samples in FSEM were obtained by means of impact Charpy testing, this means that the observed morphology observed in Fig. 7 represents the impact strength of behaviour of the samples. As it has proposed above, the best temperature for the impact properties is 120 °C, providing the best energy absorption. Those samples that have absorbed more energy during the fracture have a higher roughness promoted by a higher plastic deformation and then the surface turns flatter when the fracture is brittle due to a low plastic deformation [57,58]. Those samples cured at 130 °C show a clear decrease in the impact strength, this reduced plastic deformation is clearly observed with a flat surface which is more pronounced in Fig. 7f.

3.5. Thermal properties

After completing the proposed isothermal times for each sample, thermal characterization was conducted through a DSC and TGA program. The main thermal transitions measured by DSC within the tested range are depicted in Fig. 8 and summarized in Table 3. Additionally, the thermal stability measured by TGA is presented in Fig. 9 and Table 4.

As demonstrated in the aforementioned curing analysis, AESO/ACIN thermoset materials did not fully complete the process under the proposed conditions. Kyriakou *et al.* proposed that for thermoset materials, an exothermic peak related to the curing process and a glass transition temperature are observed, with both processes affected by the degree of conversion of the analyzed sample [59]. This behavior was also observed in the materials developed in this study. With an increase in the degree of conversion, there is a rise in the glass transition temperature and a reduction in the realized enthalpy. The glass transition temperature offers insight into the mobility of the material's chains; thus, the results indicate that increasing time and temperature enhances the degree of curing, leading to larger polymer chains. Consequently, increased chain size restricts material motion due to a higher number of bonds between different monomers [60]. In this study, the measured T_g varies from –32.2 °C for the sample cured at 110 °C for 1.5 h to 10.6 °C for a sample cured at 140 °C for 2.5 h. To provide a comparison with the T_g values measured in the developed materials, other authors have reported values close to 0 °C for epoxidized vegetable oils obtained from sources like soybean or linseed [61].

As observed in the mechanical characterization, samples cured at 140 °C exhibited a highly brittle behavior. In the thermal characterization, these samples displayed T_g values close to room temperature, which restrict the chain mobility of the material. As suggested in the mechanical characterization, the most favorable mechanical behavior is achieved in samples cured at 130 °C. The DSC characterization reveals that these samples have a glass transition temperature below 0 °C, facilitating the attainment of proper ductile properties.
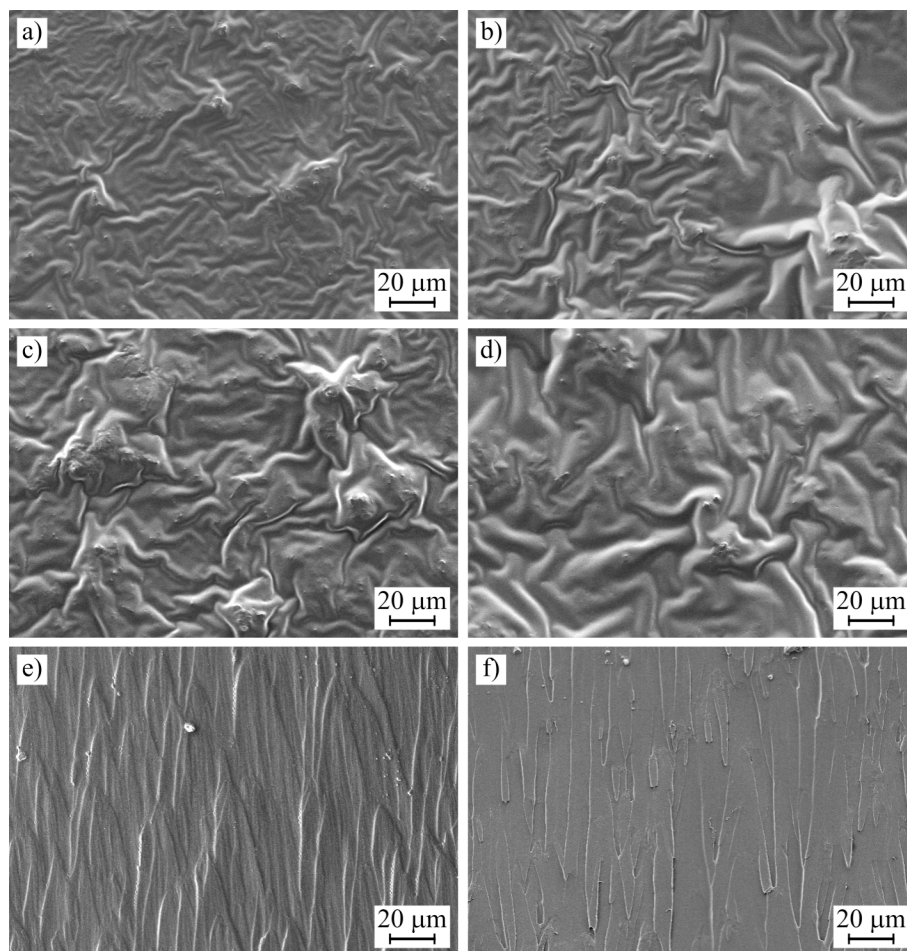
Fig. 7. Morphology of the samples fractured in Charpy impact conditions obtained by means of FSEM at × 500: a) 110/1.5, b) 110/2.5, c) 120/1.5 d) 120/2.5, e) 130/1.5 and f) 130/2.5.
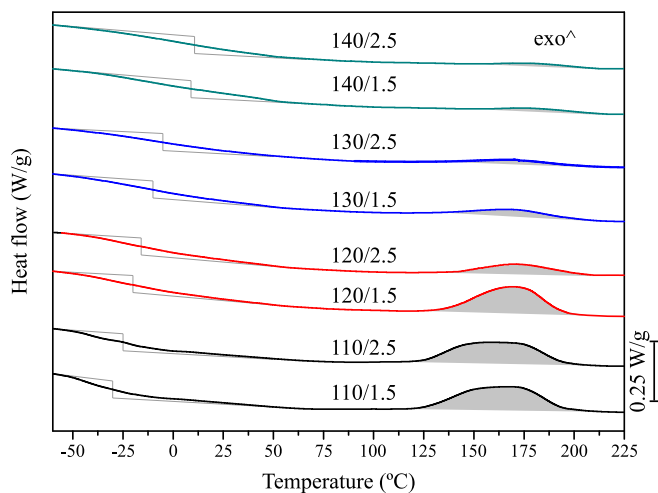

Fig. 8. DSC thermograms for the cured resins at different isothermal temperatures and times.

Table 3

Main thermal parameters obtained by means of DSC for the cured resins at different isothermal temperatures and times.

Sample	T_g (°C)	Δh(J/g)	T_p (°C)
110/1.5	−32.2 ± 0.8	30.6 ± 0.5	168.8 ± 0.8
110/2.5	−25.3 ± 0.5	28.2 ± 0.6	166.3 ± 0.5
120/1.5	−20.6 ± 0.7	24.4 ± 0.5	169.5 ± 1.1
120/2.5	−16.3 ± 0.9	10.5 ± 0.4	170.4 ± 0.6
130/1.5	−11.4 ± 1.2	7.9 ± 0.3	170.2 ± 0.7
130/2.5	−5.2 ± 1.4	3.6 ± 0.2	171.2 ± 0.9
140/1.5	9.2 ± 0.5	2.9 ± 0.2	177.5 ± 1.2
140/2.5	10.6 ± 0.8	2.0 ± 0.2	176.9 ± 1.5

monomers employed in certain applications, thereby limiting temperature dissipation [62]. For samples cured at the lowest temperature, the measure enthalpy is close to 30 J/g, this value is clearly reduced with the increase in the employed isothermal temperature. The measured values are close to 2.0 J/g for those samples cured with the most aggressive conditions.

The thermal stability of the cured resins exhibits varying behavior depending on the temperature utilized during the reticulation process. Changes in temperature during thermoset material synthesis result in a reticular network with different molecular weights. Generally, increasing the isothermal curing temperature enhances thermal stability, as higher degrees of conversion promote a more stable structure [11]. This is evident in the initial temperature degradation (T5), where lower curing temperatures lead to higher mass loss, primarily due to the
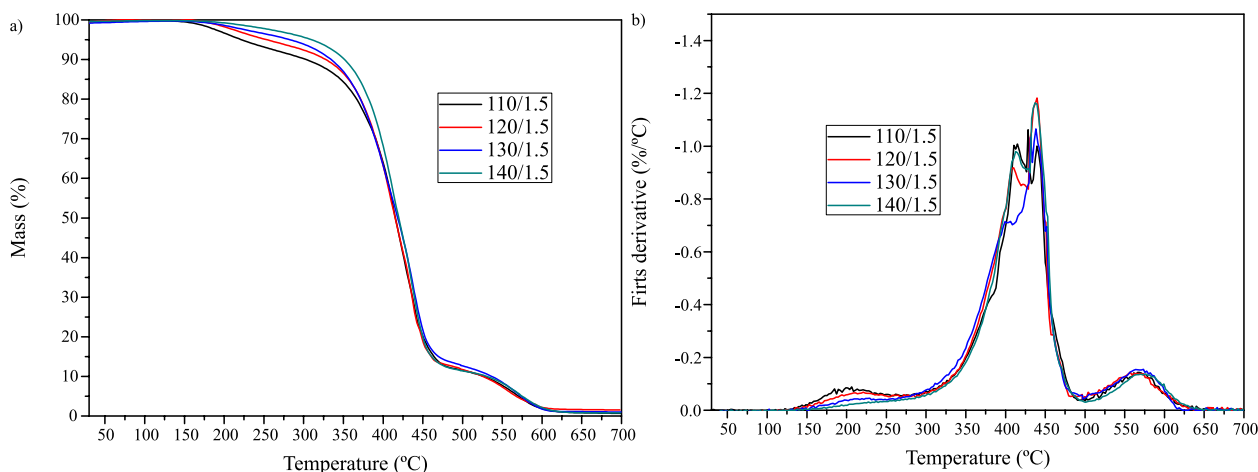
Regarding the released heat observed in the temperature range from 125 °C to 200 °C, it is attributed to the exothermic reaction occurring during the curing process. As anticipated, the amount of heat released decreases with increasing temperature. In other studies, it has been proposed that the exothermic heat generated during curing can potentially disrupt the integrity of the thermoset due to the degradation of the

Fig. 9. TGA curves for the cured resins at different isothermal temperatures for 1.5 h: a) mass loss vs temperature and b) first derivative vs temperature.

Table 4
Main thermal parameters obtained by means of TGA for the cured resins at different isothermal temperatures.

Sample	T_5 (°C)	T_{max} (°C)	Residue mass (%)
110/1.5	220.9 ± 1.2	427.2 ± 1.5	0.7 ± 0.1
120/1.5	253.7 ± 1.3	441.4 ± 1.4	0.6 ± 0.1
130/1.5	282.4 ± 0.9	436.7 ± 1.5	0.5 ± 0.1
140/1.5	308.4 ± 0.8	436.9 ± 2.2	0.6 ± 0.1

low thermal stability of ACIN, initiating the first stage of thermal decomposition attributed mainly to the volatilization of cinnamon-derived components [51]. In a study conducted by Chen *et al.*, the development of thermoset materials with AESO suggested an initial degradation temperature of 310 °C, with decomposition occurring in a single-step process [17]. In our developed thermosets, the unreacted ACIN is responsible for initiating the initial mass loss process. Moreover, for samples cured at 140 °C, this phenomenon occurs at 308.4 °C, similar to findings by Chen *et al.*, with samples cured at this temperature exhibiting the highest conversion degree, close to 90 %.

Following the initial stage of mass loss, another significant mass loss stage occurs between 300 °C and 500 °C. This second region, observed in the study by Anbinder *et al.* as well, is attributed to the conversion of the crosslinked polymer network into carbon, with the highest mass loss occurring in this range [14]. In this temperature range, the behavior of all proposed materials is quite similar, as the unreacted parts have

already been volatilized in the previous stage of the test.

Lastly, above 500 °C up to approximately 600 °C, a final stage of mass loss marks the end of the decomposition process. In this phase, the char produced in the previous stages undergoes oxidation and degradation [14]. Ultimately, these three stages result in a low residue above 600 °C, with all measured formulations exhibiting below 1 % residue.

3.6. Thermomechanical properties

The thermomechanical behavior of the developed formulations was assessed using DMTA. Fig. 10 illustrates the obtained curves, while Table 5 summarizes the most significant parameters extracted from the test. Samples cured at various temperatures for 1.5 h were analyzed to evaluate differences arising from changes in curing temperature. A single-step process was observed, wherein the storage modulus decreases with increased chain involvement in each sample, attributed to

Table 5
Main thermomechanical parameters obtained by means of DMTA for the cured resins at different isothermal temperatures.

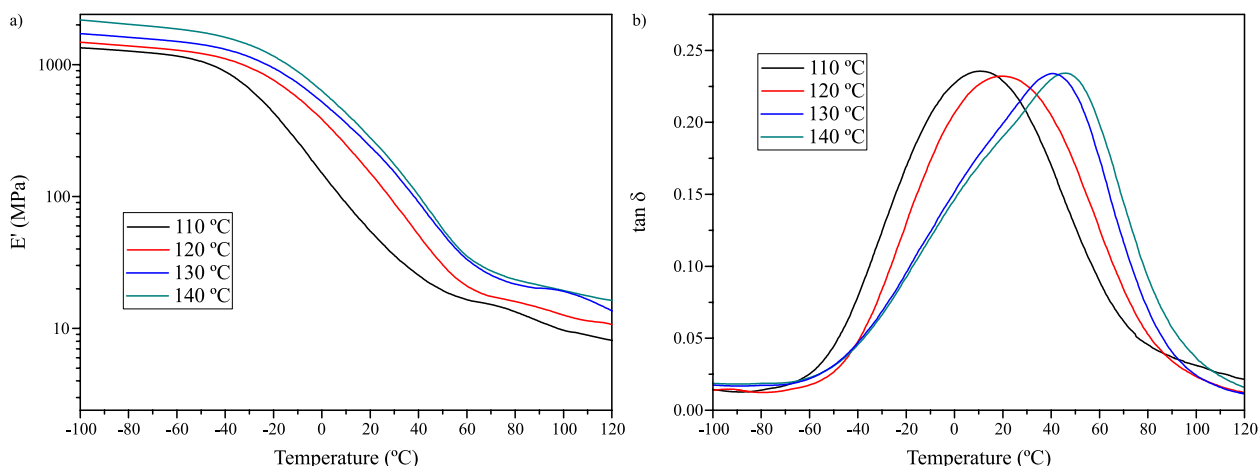| Sample	E' at −80 °C (MPa)	E' at 25 °C (MPa)	T_g (°C)
110/1.5	1238 ± 33	42.6 ± 5	11.8 ± 0.5
120/1.5	1377 ± 24	97.7 ± 4	20.3 ± 0.4
130/1.5	1620 ± 57	170.5 ± 13	42.4 ± 0.5
140/1.5	2041 ± 69	203.2 ± 21	46.7 ± 0.3

Fig. 10. DMTA curves for the cured resins at different isothermal temperatures for 1.5 h: a) storage modulus vs temperature and b) damping factor vs temperature.

an α-relaxation process linked to the glass transition temperature, as depicted in the tan δ curve. Chen *et al.* observed a similar peak, along with an additional β-relaxation peak at a lower temperature for thermoset materials developed with 2,5-furandicarboxylic acid (FDCA) [63]. he peak value in the tan δ curve can be utilized to estimate the glass transition temperature [64]. As proposed in the manuscript, increasing the curing temperature enhances the conversion degree, improving mechanical behavior and sample stiffness. Consistent with DSC findings, the glass transition temperature increases with higher curing temperatures, with the glass transition of samples cured at 110 °C measuring 11.8 °C, shifting to 46.7 °C for those cured at 140 °C. In Bertini *et al.*'s work, different biobased resins developed with AESO and terpenes obtained Tg values ranging between 49 °C and 65 °C [65].

The storage modulus of the samples is highly linked with the cross-linking networks formed as proposed by Zhen *et al.* [66].As also mentioned, the flexural properties of the samples proposed that the increase in temperature employed in the curation process promotes an increase in stiffness of the samples. This increase in terms of stiffness is observed in the DMTA at different temperatures. In Table 5 the E' values at −80 °C and 25 °C are presented. For example, 110/1.5 has 1238 MPa at −80 °C and this value increases up to 1620 MPa for 130/1.5. As mentioned, the reticular network created during the curation process has the highest effect over the final properties of the material [67]. An effect to highlight is the clear decrease int terms of E' due to the glass transition temperature, at 25 °C values are reduced to 200 MPa or lower. The developed thermoset materials at room temperature have a low stiffens as also observed in the flexural properties. Vergara *et al.* in thermoset materials developed with bisphenol a also observed a similar behavior in terms of storage modulus, showing a high stiffness at low temperatures and a very low stiffness above glass transition temperature [68].

4. Conclusions

The findings from this study have profound implications for the design of biobased thermoset materials for the future. The enhanced properties and reduced environmental impact demonstrated by AESO and allyl cinnamate provide actionable insights for material scientists and engineers looking to develop sustainable composite materials. The materials were mixed and subjected to various isothermal conditions for curing, ranging from 110 °C to 140 °C, and by varying the isothermal times. Analysis of the curing process under isothermal conditions revealed that the degree of conversion and gel fraction of the developed material increased with the temperature employed. Higher temperatures accelerated the conversion process, while lower temperatures resulted in a slower process. The formation of a reticular network at higher temperatures led to improved performance of the thermoset materials, with the highest flexural strength observed in samples cured at 130 °C for 2.5 h. However, despite this increased strength, impact properties were better for samples cured at 120 °C, a lower degree of conversion allowed for the creation of a reticular network with higher mobility. All these proposed phenomena in mechanical properties were confirmed through morphological observations using electron microscopy. The thermal characterization under dynamic conditions revealed a significant change in the glass transition temperature of the developed materials, depending on the employed curing conditions. Additionally, unreacted products reacted under dynamic conditions, resulting in an exothermic reaction. Increasing the temperature during the curing process also improved the thermal stability of the samples, attributed to the increased molecular weight of the chains. Furthermore, the thermomechanical study confirmed the observed increase in stiffness during the flexural test, as well as the increase in the glass transition temperature. The implications for design are profound. Designers and engineers are encouraged to leverage these findings to fine-tune the crosslinking density and curing parameters, tailoring the mechanical and thermal properties to meet the demands of specific applications. This could range

from automotive components to aerospace structures, where performance and environmental sustainability are paramount. Moreover, the exploration of other biobased diluents promises to broaden the spectrum of achievable properties, potentially leading to innovations in thermoset materials with even greater performance and reduced environmental footprints. This study not only shifts paradigms in material selection but also enhances the foundational knowledge required to engineer next-generation materials.

CRediT authorship contribution statement

Diego Lascano: Investigation, Conceptualization. **Jaume Gomez-Caturla:** Writing – review & editing, Writing – original draft, Investigation. **David Garcia-Sanoguera:** Validation, Supervision, Resources. **Daniel Garcia-Garcia:** Resources, Project administration, Funding acquisition, Conceptualization. **Juan Ivorra-Martinez:** Writing – review & editing, Methodology, Formal analysis, Data curation.

Declaration of competing interest

The authors declare the following financial interests/personal relationships which may be considered as potential competing interests: Dani Garcia-Garcia reports financial support was provided by Government of Valencia. Jaume Gomez Caturla reports financial support was provided by Spain Ministry of Science and Innovation. David Garcia Sanoguera reports was provided by Spain Ministry of Science and Innovation. Diego Lascano reports was provided by Government of Valencia. If there are other authors, they declare that they have no known competing financial interests or personal relationships that could have appeared to influence the work reported in this paper.

Data availability

Data will be made available on request.

Acknowledgements

References

[1] K.L. Chong, J.C. Lai, R.A. Rahman, N. Adrus, Z.H. Al-Saffar, A. Hassan, T.H. Lim, M.U. Wahit, A review on recent approaches to sustainable bio-based epoxy vitrimer from epoxidized vegetable oils, Ind. Crops Prod. 189 (1) (2022) 115857.

[2] A.R. Schmidt, A.P. Dresch, S.L. Alves Junior, J.P. Bender, H. Treichel, Applications of brewer's spent grain hemicelluloses in biorefineries: Extraction and value-added product obtention, Catalysts 13 (4) (2023) 755–776.

[3] F. Chemat, M.A. Vian, H.K. Ravi, Toward petroleum-free with plant-based chemistry, Curr. Opin. Green Sustain. Chem. 28 (1) (2021) 100450.

[4] D. Zorko, I. Demšar, J. Tavčar, An investigation on the potential of bio-based polymers for use in polymer gear transmissions, Polym Test 93 (1) (2021) 106994.

[5] A. Perez-Nakai, A. Lerma-Canto, A. Trejo-Machín, I. Dominguez-Candela, J. Miguel Ferri, V. Fombuena, Assessing novel thermoset materials from brazil nut oil: Curing, thermal and mechanical properties, EXPRESS Polym. Lett. 17 (12) (2023) 1224–1238.

[6] J. Liu, L. Zhang, W. Shun, J. Dai, Y. Peng, X. Liu, Recent development on bio-based thermosetting resins, J. Polym. Sci. 59 (14) (2021) 1474–1490.

[7] T. Liu, B. Zhao, J. Zhang, Recent development of repairable, malleable and recyclable thermosetting polymers through dynamic transesterification, Polymer 194 (1) (2020) 1–16.

[8] S. Zhou, K. Huang, X. Xu, B. Wang, W. Zhang, Y. Su, K. Hu, C. Zhang, J. Zhu, G. Weng, S. Ma, Rigid-and-flexible, degradable, fully biobased thermosets from lignin and soybean oil: Synthesis and properties, ACS Sustain. Chem. Eng. 11 (8) (2023) 3466–3473.

[9] D. Lascano, C. Aljaro, E. Fages, S. Rojas-Lema, J. Ivorra-Martinez, N. Montanes, Study of the mechanical properties of polylactide composites with jute reinforcements, Green Mater. 40 (2022) 1–10.

[10] V. Chaudhary, F. Ahmad, A review on plant fiber reinforced thermoset polymers for structural and frictional composites, Polym Test 91 (1) (2020) 106792.

[11] Y. Liu, F. Lu, N. Xu, B. Wang, L. Yang, Y. Huang, Z. Hu, Mechanically robust, hydrothermal aging resistant, imine-containing epoxy thermoset for recyclable carbon fiber reinforced composites, Mater. Des. 224 (1) (2022) 111357.

[12] J. Wan, J. Zhao, X. Zhang, H. Fan, J. Zhang, D. Hu, P. Jin, D.Y. Wang, Epoxy thermosets and materials derived from bio-based monomeric phenols: Transformations and performances, Prog. Polym. Sci. 108 (1) (2020) 101287.

[13] S. Kumar, S. Krishnan, S. Mohanty, S.K. Nayak, Synthesis and characterization of petroleum and biobased epoxy resins: a review, Polym. Int. 67 (7) (2018) 815–839.

[14] S. Anbinder, C. Meiorin, C. Macchi, M.A. Mosiewicki, M.I. Aranguren, A. Somoza, Structural properties of vegetable oil thermosets: Effect of crosslinkers, modifiers and oxidative aging, Eur Polym J 124 (1) (2020) 109470.

[15] X.M. Ding, L. Chen, D.M. Guo, B.W. Liu, X. Luo, Y.F. Lei, H.Y. Zhong, Y.Z. Wang, Controlling cross-linking networks with different imidazole accelerators toward high-performance epoxidized soybean oil-based thermosets, ACS Sustain. Chem. Eng. 9 (8) (2021) 3267–3277.

[16] S.S. Hashemi, D. Mondal, J. Montesano, T.L. Willett, Effects of biopolymer functionalization and nanohydroxyapatite heat treatment on the tensile and thermomechanical properties of bone-inspired 3D printable nanocomposite biomaterials, Mater. Des. 225 (1) (2023) 111587.

[17] J. Chen, H. Liu, W. Zhang, L. Lv, Z. Liu, Thermosets resins prepared from soybean oil and lignin derivatives with high biocontent, superior thermal properties, and biodegradability, J. Appl. Polym. Sci. 137 (26) (2020) 1–11.

[18] J. Pansumdaeng, S. Kuntharin, V. Harnchana, N. Supanchaiyamat, Fully bio-based epoxidized soybean oil thermosets for high performance triboelectric nanogenerators, Green Chem. 22 (20) (2020) 6912–6921.

[19] F. Gapsari, D.B. Darmadi, H. Juliano, S. Hidayatullah, S.M. Suteja, S.S. Rangappa, Modification of palm fiber with chitosan-AESO blend coating, Int. J. Biol. Macromol. 242 (1) (2023) 125099.

[20] X. Yang, L. Guo, X. Xu, S. Shang, H. Liu, A fully bio-based epoxy vitrimer: Self-healing, triple-shape memory and reprocessing triggered by dynamic covalent bond exchange, Mater. Des. 186 (1) (2020) 108248.

[21] M.A. Hofmann, A.T. Shahid, M. Garrido, M.J. Ferreira, J.R. Correia, J.C. Bordado, Biobased thermosetting polyester resin for high-performance applications, ACS Sustain. Chem. Eng. 10 (11) (2022) 3442–3454.

[22] P. Spasojevic, S. Seslija, M. Markovic, O. Pantic, K. Antic, M. Spasojevic, Optimization of reactive diluent for bio-based unsaturated polyester resin: A rheological and thermomechanical study, Polymers 13 (16) (2021) 2667.

[23] Y. Zhang, Y. Li, L. Wang, Z. Gao, M.R. Kessler, Synthesis and characterization of methacrylated eugenol as a sustainable reactive diluent for a maleinated acrylated epoxidized soybean oil resin, ACS Sustain. Chem. Eng. 5 (10) (2017) 8876–8883.

[24] A.R. Jagtap, A. More, Developments in reactive diluents: a review, Polym. Bull. 79 (8) (2022) 5667–5708.

[25] I. Hevus, P. Kannaboina, Y. Qian, J. Wu, M. Johnson, L.R. Gibbon, J.J.L. Scala, C. Ulven, M.P. Sibi, D.C. Webster, Furanic (meth) acrylate monomers as sustainable reactive diluents for stereolithography, ACS Appl. Polym. Mater. 5 (11) (2023) 9659–9670.

[26] T. Luo, Y. Ma, X. Cui, Review on frontal polymerization behavior for thermosetting resins: materials, modeling and application, Polymers 16 (2) (2024) 185.

[27] C.D. Varganici, L. Rosu, S. Lehner, C. Hamciuc, M. Jovic, D. Rosu, F. Mustata, S. Gaan, Semi–interpenetrating networks based on epoxy resin and oligophosphonate: Comparative effect of three hardeners on the thermal and fire properties, Mater. Des. 212 (1) (2021) 110237.

[28] H. Fang, C.A. Guymon, Recent advances to decrease shrinkage stress and enhance mechanical properties in free radical polymerization: A review, Polym. Int. 71 (5) (2022) 596–607.

[29] Z. Fang, X. Wu, X. Zhu, C. Luo, D. Li, Q. Liu, K. Wang, Curing kinetics study of thermosetting resin material with ultra-low dielectric loss for advanced electronic packaging, Polym Test 130 (1) (2024) 108312.

[30] J. Kruželák, R. Sýkora, I. Hudec, Vulcanization of rubber compounds with peroxide curing systems, Rubber Chem. Technol. 90 (1) (2016) 60–88.

[31] D. Lascano, A. Lerma-Canto, V. Fombuena, R. Balart, N. Montanes, L. Quiles-Carrillo, Kinetic analysis of the curing process of biobased epoxy resin from epoxidized linseed oil by dynamic differential scanning calorimetry, Polymers 13 (8) (2021) 1279.

[32] X. Zhang, Y. Wu, J. Wei, J. Tong, X. Yi, Curing kinetics and mechanical properties of bio-based composite using rosin-sourced anhydrides as curing agent for hot-melt prepreg, Sci. China Technol. Sci. 60 (9) (2017) 1318–1331.

[33] C. Monteserin, M. Blanco, J.M. Laza, E. Aranzabe, J.L. Vilas, Thickness effect on the generation of temperature and curing degree gradients in epoxy–amine thermoset systems, J. Therm. Anal. Calorim. 132 (1) (2018) 1867–1881.

[34] A. Anusic, Y. Blößl, G. Oreski, K. Resch-Fauster, High-performance thermoset with 100% bio-based carbon content, Polym. Degrad. Stab. 181 (1) (2020) 109284.

[35] C. Lu, Y. Liu, C. Wang, Q. Yong, J. Wang, F. Chu, An integrated strategy to fabricate bio-based dual-cure and toughened epoxy thermosets with photothermal conversion property, J. Chem. Eng. 433 (1) (2022) 134582.

[36] Y. Zhang, F. Ma, L. Shi, B. Lyu, J. Ma, Recyclable, repairable and malleable bio-based epoxy vitrimers: overview and future prospects, Curr. Opin. Green Sustain. Chem. 39 (1) (2023) 100726.

[37] C. Zhang, M. Yan, E.W. Cochran, M.R. Kessler, Biorenewable polymers based on acrylated epoxidized soybean oil and methacrylated vanillin, Materials Today Communications 5 (1) (2015) 18–22.

[38] T.H. Thi, M. Matsusaki, D. Shi, T. Kaneko, M. Akashi, Synthesis and properties of coumaric acid derivative homo-polymers, Journal of Biomaterials Science, Polymer Edition 19 (1) (2008) 75–85.

[39] O. Karthaus, Y. Hashimoto, K. Kon, Y. Tsuriga, Solvent Resistant Honeycomb Films from Photo-Crosslinkable Polycinnamate, Macromolecular Rapid Communications 28 (8) (2007) 962–965.

[40] M. Imada, Y. Takenaka, H. Hatanaka, T. Tsuge, H. Abe, Unique acrylic resins with aromatic side chains by homopolymerization of cinnamic monomers, Communications Chemistry 2 (2019).

[41] C. Marvel, G. McCain, Polymerization of Esters of Cinnamic Acid1, Journal of the American Chemical Society 75 (13) (1953) 3272–3273.

[42] E.S. Beach, Z. Cui, P.T. Anastas, M. Zhan, R.P. Wool, Properties of thermosets derived from chemically modified triglycerides and bio-based comonomers, Applied Sciences 3 (4) (2013) 684–693.

[43] J. Grimalt, L. Frattini, P. Carreras, V. Fombuena, Optimizing rheological performance of unsaturated polyester resin with bio-based reactive diluents: A comprehensive analysis of viscosity and thermomechanical properties, Polym Test 129 (1) (2023) 108264.

[44] W. Liu, M.-E. Fei, Y. Ban, A. Jia, R. Qiu, Preparation and evaluation of green composites from microcrystalline cellulose and a soybean-oil derivative, Polymers 9 (10) (2017) 541.

[45] M. Fernandes, A.P. Souto, M. Gama, F. Dourado, Bacterial cellulose and emulsified AESO biocomposites as an ecological alternative to leather, Nanomaterials 9 (12) (2019) 1710.

[46] W. Li, Q. Zhan, P. Yang, Facile approach for the synthesis of performance-advantaged degradable bio-based thermoset via ring-opening metathesis polymerization from epoxidized soybean oil, ACS Sustain. Chem. Eng. 11 (3) (2023) 1200–1206.

[47] A.E. Klingbeil, J.B. Jeffries, R.K. Hanson, Temperature-dependent mid-IR absorption spectra of gaseous hydrocarbons, J QUANT SPECTROSC RA 107 (3) (2007) 407–420.

[48] F. Li, T.S.Y. Choong, L. Soltani, L. Chuah Abdullah, S.N.A.M. Jamil, N.n., Amerhaider Nuar, Investigation of glyphosate removal from aqueous solutions using fenton-like system based on calcium peroxide, Processes 10 (10) (2022) 2045.

[49] Z. Su, K. Zhao, Z. Ye, W. Cao, X. Wang, K. Liu, Y. Wang, L. Yang, B. Dai, J. Zhu, Overcoming the penetration–saturation trade-off in binder jet additive manufacturing via rapid in situ curing, Addit. Manuf. 59 (1) (2022) 103157.

[50] C. Di Mauro, S. Malburet, A. Genua, A. Graillot, A. Mija, Sustainable series of new epoxidized vegetable oil-based thermosets with chemical recycling properties, Biomacromolecules 21 (9) (2020) 3923–3935.

[51] A. Barandiaran, J. Gomez-Caturla, J. Ivorra-Martinez, D. Lascano, M.A. Selles, V. Moreno, O. Fenollar, Esters of cinnamic acid as green plasticizers for polylactide formulations with improved ductility, Macromol. Mater. Eng. 308 (8) (2023) 2300022.

[52] T. Sivasankaraiah, B.R. Lokavarapu, J.V. Rajesh, Post-curing effect on flexural strength of glass epoxy composites, Mater. Today Proc. 38 (1) (2021) 3320–3331.

[53] X. Wan, B. Demir, M. An, T.R. Walsh, N. Yang, Thermal conductivities and mechanical properties of epoxy resin as a function of the degree of cross-linking, Int. J. Heat Mass Transf. 180 (1) (2021) 121821.

[54] G. Daissè, M. Marcon, M. Zecchini, R. Wan-Wendner, Cure-dependent loading rate effects on strength and stiffness of particle-reinforced thermoset polymers, Polymer 259 (1) (2022) 125326.

[55] I. Ribca, M.E. Jawerth, C.J. Brett, M. Lawoko, M. Schwartzkopf, A. Chumakov, S. V. Roth, M. Johansson, Exploring the effects of different cross-linkers on lignin-based thermoset properties and morphologies, ACS Sustain. Chem. Eng. 9 (4) (2021) 1692–1702.

[56] Y. Li, L. Yuan, G. Liang, A. Gu, Developing Reprocessable shape memory thermosetting resins with high thermal resistance and strength through building a crosslinked network based on bismaleimide and epoxy resins, J. Appl. Polym. Sci. 140 (13) (2023) e53685.

[57] J. Gomez-Caturla, R. Balart, J. Ivorra-Martinez, D. Garcia-Garcia, F. Dominici, D. Puglia, L. Torre, Biopolypropylene-based wood plastic composites reinforced with mango peel flour and compatibilized with an environmentally friendly copolymer from itaconic acid, ACS Appl. Polym. Mater. 4 (6) (2022) 4398–4410.

[58] R. Tejada-Oliveros, J. Gomez-Caturla, O. Fenollar, N. Montanes, J. Ivorra-Martinez, D. Garcia-Garcia, Assessment of non-ester monoterpenoids as biobased plasticizers for polylactide with improved ductile behaviour, Polymer 290 (1) (2024) 126572.

[59] C.K. Tziamtzi, K. Chrissafis, Optimization of a commercial epoxy curing cycle via DSC data kinetics modelling and TTT plot construction, Polymer 230 (1) (2021) 124091.

[60] D.J. Dobbins, G.M. Scheutz, H. Sun, C.A. Crouse, B.S. Sumerlin, Glass-transition temperature governs the thermal decrosslinking behavior of Diels-Alder crosslinked polymethacrylate networks, J. Polym. Sci. 58 (1) (2020) 193–203.

[61] J. Thomas, J. Nwosu, M.D. Soucek, Acid-cured norbornylized seed oil epoxides for sustainable, recyclable, and reprocessable thermosets and composite application, ACS Appl. Polym. Mater. 5 (3) (2023) 2230–2242.

[62] Z. Ran, X. Liu, X. Jiang, Y. Wu, H. Liao, Study on curing kinetics of epoxy-amine to reduce temperature caused by the exothermic reaction, Thermochim. Acta 692 (1) (2020) 178735.

[63] X. Chen, S. Chen, Z. Xu, J. Zhang, M. Miao, D. Zhang, Degradable and recyclable bio-based thermoset epoxy resins, Green Chem. 22 (13) (2020) 4187–4198.

[64] D. Lascano, R. Balart, D. Garcia-Sanoguera, A. Agüero, T. Boronat, N. Montanes, Manufacturing and characterization of hybrid composites with basalt and flax fabrics and a partially bio-based epoxy resin, Fibers Polym. 22 (1) (2021) 751–763.

[65] F. Bertini, A. Vignali, M. Marelli, N. Ravasio, F. Zaccheria, Styrene-free bio-based thermosetting resins with tunable properties starting from vegetable oils and terpenes, Polymers 14 (19) (2022) 4185.

[66] X. Zhen, H. Li, Z. Xu, Q. Wang, S. Zhu, Z. Wang, Z. Yuan, Facile synthesis of lignin-based epoxy resins with excellent thermal-mechanical performance, Int. J. Biol. Macromol. 182 (1) (2021) 276–285.

[67] Q. Cao, J. Li, Y. Qi, S. Zhang, J. Wang, Z. Wei, H. Pang, X. Jian, Z. Weng, Engineering double load-sharing network in thermosetting: Much more than just toughening, Macromolecules 55 (21) (2022) 9502–9512.

[68] J.H. Vergara, S.K. Yadav, O. Bolarin, J.J. La Scala, G.R. Palmese, Synthesis and characterization of low-viscosity bio-based styrene alternatives for bisphenol a vinyl ester thermosetting resins, ACS Sustain. Chem. Eng. 8 (46) (2020) 17234–17244.